TELLUS

Cloud droplet activation of polymerized organic aerosol

By MARKUS D. PETTERS[1*], SONIA M. KREIDENWEIS[1], JEFFERSON R. SNIDER[2], KIRSTEN A. KOEHLER[1], QIANG WANG[3], ANTHONY J. PRENNI[1] and PAUL J. DEMOTT[1],
[1]*Department of Atmospheric Science, Colorado State University, Fort Collins CO, 80523, USA;* [2]*Department of Atmospheric Science, University of Wyoming, Laramie WY, 82071, USA;* [3]*Department of Chemical Engineering, Colorado State University, Fort Collins, CO 80523, USA*

ABSTRACT

High-molecular-weight organic compounds represent an important fraction in atmospheric aerosols, but their interactions with atmospheric water vapour are not well understood. Specifically, the hygroscopicity of polymerized atmospheric aerosols is larger than expected for their high molecular weights and is not a strong function of the degree of polymerization, but their cloud-nucleating activity declines as polymerization progresses. We apply a Flory–Huggins based theory for polymer–water interactions to describe water activity in aqueous solutions of atmospherically relevant oligomers and polymers, and show via experiments on particles composed of commercial polymers that it is consistent with observed particle hygroscopic growth and cloud formation behaviour.

1. Introduction

The nature and origin of the organic fraction of ambient particulate matter in urban and remote locations has been a longstanding question in atmospheric chemistry. In many regions, organic material dominates the ambient aerosol mass, and the corresponding role of organic aerosols in cloud formation has spurred increasing interest in theories that link their physicochemical properties, such as morphology and composition, with their cloud forming ability (Bilde and Svenningsson, 2004). Such theories are needed to evaluate direct and cloud radiative forcing that organic aerosols impart on the global climate system (IPCC, 2001). Organic particulate matter is known to have a multitude of sources, including direct emissions from the combustion of fuels and formation of secondary organic aerosol (SOA) from anthropogenic and biogenic gaseous precursors. It has been shown that high-molecular-weight organic compounds are present in marine aerosol (Cini et al., 1996), urban and rural aerosol (Decesari et al., 2001; Limbeck et al., 2003), and fog water samples (Herckes et al., 2002; Feng and Möller, 2004), and can represent significant fractions of the total organic aerosol mass. Early work identified these aerosol constituents as humic-like substances (HULIS), based on similarities in molecular weight, spectroscopy, and elemental composition, although it was recognized that, unlike humic and fulvic acids, they are not soil derived. Recent experiments (Gao et al., 2004; Kalberer et al., 2004;

Baltensperger et al., 2005) have shown that about half of the SOA produced in smog chamber experiments from the oxidation of aromatic compounds is composed of oligomers (Baltensperger et al., 2005). Although much progress has been made in understanding the nature of these atmospheric macromolecules and in proposing atmospheric reaction pathways that form them, some important properties remain unexplained.

Of particular relevance to atmospheric processes is the water associated with such macromolecules in particles exposed to varying ambient relative humidities (RHs). Equilibrium water contents have been measured for a variety of naturally formed and synthesized macromolecules. Brooks et al. (2004) measured the hygroscopic growth of particles generated from reference humic substances and from aqueous solutions of poly(acrylic acid) (PAA) of two different molecular weights, and found similar water uptake for all materials, and a weak dependence on the molecular weight or degree of polymerization of the PAA. Baltensperger et al. (2005) observed that hygroscopic growth factors of laboratory-generated SOA aerosol increased over the first 7 hr of the experiment, but then remained constant for over 20 hr, despite evidence that oligomerization continued during the entire period, reaching molecular weights as high as 1 kg mole^{-1}. In contrast, progressive oligomerization appeared to decrease the cloud-forming potential of SOA in other experiments (VanReken et al., 2005). The degree of polymerization of fulvic acid is thought to be less than humic acid (Manahan, 2000) but the hygroscopic growth below 100% RH is very similar for reference humic and fulvic acids of different origin (Chan and Chan, 2003; Brooks et al., 2004; Gysel et al., 2004) and also similar to those observed for SOA-derived oligomers (Baltensperger

et al., 2005). These observations are at odds with traditional treatments of aerosol water uptake, grounded in Raoult's law. Although Raoult's law applies only to ideal solutions, and thus at best only to dilute atmospherically relevant solutions such as those found in cloud droplets, the basic assumption has been that solution water activity scales with the mole fraction of water. Thus, the equilibrium aerosol water content at a particular RH is expected to be dependent on the molecular weight and degree of dissociation of the solute. Even taking into account the possibility of highly non-ideal solution behaviour, it is difficult to explain the unexpectedly large and surprisingly similar equilibrium water contents below 100% RH that are observed for these varied polymers and oligomers.

In this work, we examine the hygroscopic growth of two commercial polymers, poly(ethylene glycol) (PEG) and PAA, with results for the latter reported earlier by Brooks et al. (2004). Using what we will call semi-empirical Flory-Huggins/Köhler (FHK) theory, we explain the larger than anticipated hygroscopic growth and can also predict the cloud condensation nucleus activity within the uncertainties of our measurements. Although the extent of polymerization is known to reduce the solubility of the polymer, water uptake characteristics are only weakly affected. We conclude with a discussion of how limited solubility may affect hygroscopic growth and formation of cloud droplets.

2. Experimental

We examine the hygroscopic growth of two commercial polymers, PEG and PAA. Both PEG and PAA are polycarboxylic acids and thus they resemble HULIS, but it is understood that the composition of organic polymers in atmospheric aerosol is unclear to date. Both PEG and PAA are commercially available in various molecular weights and soluble in water in all proportions. Independent measurements of water activity (PAA and PEG), solution density as a function of composition (PEG) and surface tension (PEG) are available in the literature as independent tests of our method.

2.1. Water uptake measurements

A polydispersion of polymer particles was generated by atomization of an aqueous solution (TSI 3076), followed by drying (TSI 3062), and subsequent dilution with filtered dry air. Hygroscopic growth factors were measured using a hygroscopic tandem differential mobility analyser (HTDMA), which has been used previously in our laboratory (Brechtel and Kreidenweis, 2000; Prenni et al., 2003; Brooks et al., 2004) and in field studies (Carrico et al., 2005). In brief, the instrument consists of two differential mobility analysers (TSI 3071 DMA) and a humidification system. Initially, the dry polydisperse particles enter the first DMA and are made nearly monodisperse ($D = 0.1$ μm, sheath-to-monodisperse flow ratio of 5:1). Then, the monodisperse flow is brought to a controlled RH inside a Nafion (Perma

Pure Inc.) tube. Finally, the wet size distribution is measured using the second DMA (sheath-to-monodisperse flow ratio 5:1). The resulting size distributions were fit to a theoretical model accounting for the instrument transfer functions using the inversion algorithm of Zhou et al. (2002) based on the original work by Rader and McMurry (1986). From these fits we inferred the hygroscopic growth factor, g, the ratio of the equilibrium diameter at the indicated RH to that measured at RH = 5%. This method yields an overall uncertainty in g of ± 0.02 in absolute units (Carrico et al., 2005).

Prior to our measurements we modified the instrument to include a second humidification loop similar to the setup used by Mochida and Kawamura (2004). The dry, nearly monodisperse aerosol flow is diverted through a saturator (a glass flask filled with deionized water heated to $\sim 40°$ C) to raise the humidity close to water saturation. The RH at the outlet of the saturator exceeded 97%. This modification allowed better control over the RH inside the Nafion tube and increased the dynamic range of the instrument (RH = 0–96%). Using this setup we measured the dehumidification branch of the growth curve.

2.2. Cloud-condensation nuclei measurements

The critical supersaturation ($S_c = $ RH $-$ 100%) of PAA was measured using a University of Wyoming static thermal diffusion cloud chamber. A description that includes the method for calibration, both for concentration and supersaturation, is provided in Snider et al. (2003). In brief, upward vertical gradients of moisture and temperature are imposed causing water vapour supersaturations to maximize close to the mid-plane of the cloud chamber. Particles with a critical supersaturation less than that in the centre of the chamber activate and grow to the size of cloud droplets. The growth of the droplets is monitored by measuring the scattered light intensity at a scattering angle of 45° from the mid-plane region of the chamber. The two calibrations establish relationships between the peak scattered intensity and the nucleated aerosol concentration, and between the prescribed top-to-bottom temperature difference and the effective chamber supersaturation.

2.3. Test aerosol preparation

Our determinations of the critical supersaturation of PAA proceeded in the following manner. The dried polydisperse aerosol was made nearly monodisperse using a DMA (TSI 3071, sheath-to-monodisperse flow ratio of 10:1) and CCN concentration was measured at five values of effective chamber supersaturation ($s = 0.24\%, 0.48\%, 0.72\%, 0.96\%, 1.08\%$). Total aerosol concentration ([CN]) was measured by a condensation particle counter (CPC, TSI 3010). We define S_c as the supersaturation where the activated fraction equals 0.5 and determined this value from a fit of activated fraction, defined as [CCN]/[CN], versus the effective chamber supersaturation.

3. RESULTS

Figure 1 summarizes the hygroscopic behaviour observed for two different molecular weights of PAA and PEG. From Fig. 1, it is apparent that while the monomer type has some influence on the hygroscopic growth, the degree of polymerization has little effect. Also shown in Fig. 1 are data for laboratory-generated SOA from Baltensperger et al. (2005). The SOA growth factors are very similar to those of PAA over a wide range of RHs. In contrast, hygroscopic growth factors predicted by Raoult's law (hereafter designated as Raoult/Köhler or RK theory, *cf*. Appendix A.1), assuming the solute to be infinitely soluble and non-dissociating and to have a molecular weight of 2 kg mol^{-1}, indicate very little water uptake (Fig. 1). Only molecular weights on the order of 0.5 kg mol^{-1} would lead to water contents comparable to those observed, under the assumption of applicability of Raoult's law. Virtually no water uptake is predicted for an infinitely soluble and non-dissociating solute of molecular weight 3 000 kg mol^{-1}.

Mole-fraction-based water activity relationships were recognized some time ago as inadequate for describing the behaviour of solutions in which the solvent and solute molecules have very different sizes. When the molecular size of the solute is large compared to the solvent, the mole fraction of water in solution approaches unity but the water activity does not. Alternative descriptions based on lattice models, having volume fraction as the independent variable, are more appropriate (Prausnitz et al.,

Fig. 1. Hygroscopic growth factor of PEG ($\square$ 0.6 kg mol^{-1}; $\blacktriangledown$ 3.4 kg mol^{-1}) and PAA (Brooks et al., 2004) ($\diamond$, 2 kg mol^{-1}; $\bullet$ 3,000 kg mol^{-1}) as measured by the HTDMA at $T = 303$ K and water uptake of SOA ($\blacktriangle$) generated in a smog chamber (Baltensperger et al., 2005). The boxes at $RH = 90\%$ indicate the precision of the growth factor and RH measurements. The abbreviation FHK and RK denote Flory–Huggins/Köhler and Raoult/Köhler theory.

1999). Flory–Huggins theory (Flory, 1953; Prausnitz et al., 1999) and its modifications have been widely used to describe the solution behaviour of macromolecules, but its application to aerosol behaviour is not generally considered. For a binary aqueous solution containing a water-miscible solute,

$$\ln a_{\mathrm{w}} = \ln(1 - \phi) + \left(1 - \frac{1}{f}\right)\phi + \chi\phi^2, \tag{1}$$

where a_{w} is the water activity, ϕ is the volume fraction of polymer ($\phi = g^{-3}$), f is the chain segment number and is calculated in practice as the ratio of the molecular volumes of the polymer and solvent, and χ is the semi-empirical Flory–Huggins interaction parameter. The chain segment number also characterizes the degree of polymerization. The Flory–Huggins expression reduces to Raoult's law in the limit of equal molecular volumes ($f = 1$), $\chi = 0$, and zero volume change of mixing. Even when the interaction parameter is zero, large negative deviations from Raoult's law occur simply due to differences in molecular sizes of solvent and solute (Prausnitz et al., 1999). This implies that water vapour pressure over such solutions is suppressed relative to Raoult's law and that higher water contents are required to establish equilibrium with a given ambient RH, consistent with the experimental observations described in Section 1.

As can be seen from eq. (1), the water activity in aqueous polymer solutions is a strong function of segment number for small values of f, but becomes essentially independent of f as f becomes large. Such behaviour is consistent with observations suggesting minimal dependence of SOA water content on degree of polymerization after polymerization has proceeded to a certain extent (Baltensperger et al., 2005).

It is known that χ is dependent on solution composition, but methods for predicting χ from first principles or by using functional group contributions as is done in UNIFAC (e.g. Raatikainen and Laaksonen, 2005) are not yet available and thus we assume that the interaction parameter varies with polymer volume fraction according to Wolf (2003) and use our HTDMA data to fit the adjustable parameters:

$$\chi \approx \frac{\psi}{(1 - \nu\phi)^2} - \beta(1 + 2\phi), \tag{2}$$

where $\psi = \chi_0 + \beta$, χ_0 is the Flory–Huggins interaction parameter at infinite dilution, β is the conformational relaxation of the polymer due to the insertion of solvent molecules, and ν accounts for surface and entropy effects on χ. Although χ may depend on molecular weight even for concentrated solutions (Brandrup et al., 2004; p. VII/250), we assume that a χ-ϕ expression derived for one molecular weight applies for all degrees of polymerization. We note that eqs (1) and (2) do not strictly apply to polyelectrolytes that contain ionizable groups. Pure PAA is a weak polyacid and the contribution of the hydrogen ions to the total water activity is small (Appendix A.2). Therefore, we also assume that eqs (1) and (2) are adequate for fitting our data for PAA solutions.
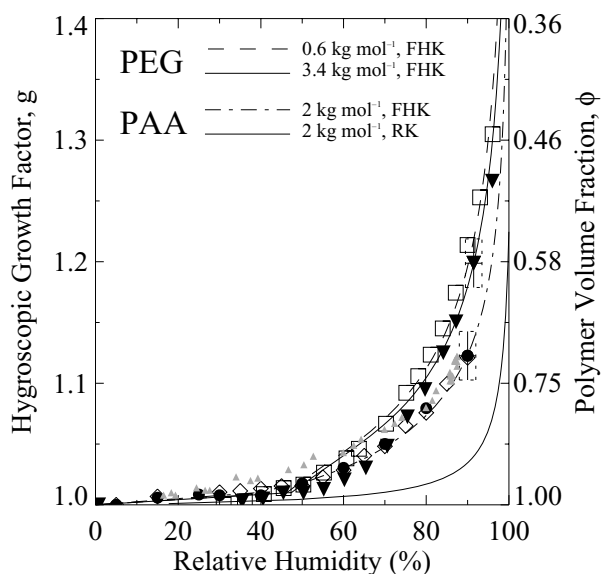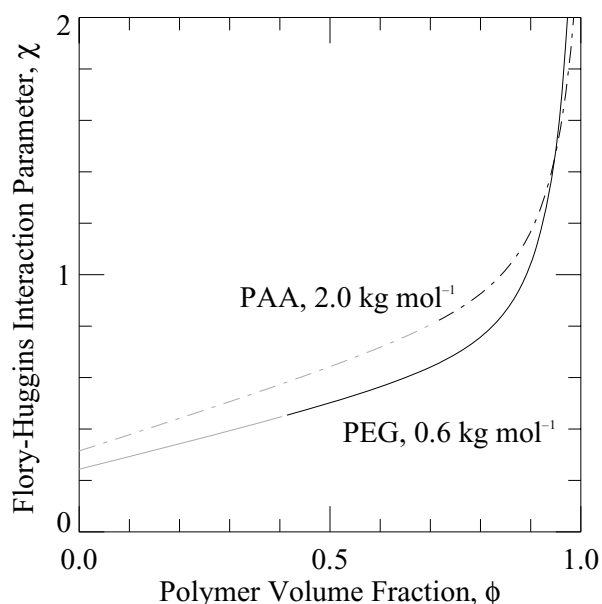
Fig. 2. Variation of the semi-empirical Flory–Huggins interaction parameter with volume fraction, based on a fit to eq. (2). The light grey shading indicates the extrapolation of the fit beyond our data.

We determine best-fit values of ψ, β and v in a two-step procedure: first we calculate water activity as a function of polymer volume fraction from the measurement of g versus RH using Köhler theory (Seinfeld and Pandis, 1998),

$$a_w = (RH/100)/\exp\left(\frac{4\sigma_{s/a}M_w}{\rho_w RT D}\right) \tag{3}$$

This equation, and variations of it for mixed-solute particles, are widely applied to predict water uptake and the *RH* of cloud droplet formation. In eq. (3), $\sigma_{s/a}$ is the surface tension of the solution/air interface and is a function of composition (Langmuir, 1917; Facchini et al., 1999, Appendix A.3), M_w is the molecular weight of water, ρ_w is the density of pure water, R is the universal gas constant, T is temperature and D is the droplet diameter. We then obtain a value of χ for each obser-

vation using eq. (1) and calculate ψ, β and v through minimization of the chi-square statistic. The relationships thus obtained are shown in Fig. 2. The lighter shading indicates volume fractions where χ values are extrapolated beyond our data. The parameters ψ, β, v and eqs (1)–(3), together with the surface tension relationships developed in Appendix A.3, define equilibrium particle water contents for what we will refer to as FHK theory. The approach and parameters are summarized in Table 1. Calculated water uptake according to FHK theory (Fig. 1) indicates that the fit equations are representative of the experimental observations.

In Fig. 3 we compare our derived volume fraction–water activity relationships with water activity data reported for PEG (0.6 kg mol^{-1}) (Gaube et al., 1993) and PAA (4 kg mol^{-1}) (Safronov et al., 1993), using a variety of standard analytical techniques. The results are generally in very good agreement. A small difference at high polymer volume fractions between the inferred water activity for PEG and previously reported values (Gaube et al., 1993) can be explained by experimental errors at low g, as seen in the solid line where we have assumed that the reference dry diameter was biased low by 2%, representative of our experimental uncertainty.

In Fig. 4 we show results from our CCN measurements of dry 0.097 μm diameter PAA (2 kg mol^{-1}) aerosol. Based on a fit of an error function to these data we inferred that the critical supersaturation was 0.53 ± 0.06%. This value is compared to predicted critical supersaturations in Fig. 5, where we extend eq. (3), combined with the Flory–Huggins' or Raoult's water activity relationship, into the water-supersaturated region. Although the curves for FHK and RK theory exhibit different growth at $RH < 100$%, the predicted maxima of the curves, that is, the critical supersaturations S_c, are comparable and lie within the experimental uncertainty. The measured critical supersaturation is in reasonable agreement with either prediction.

We assumed an osmotic coefficient of unity as input for RK theory (Appendix A.1) and thus we ignored non-ideal effects of the solute. One way to account for such effects is to fit the growth factor data to the functional form suggested by Kreidenweis et al.

Table 1. Summary of Flory–Huggins Köhler theory

	Measured quantities			Fitted parameters $\chi(\phi)$			Extrapolation	
	$g(RH)$	$\sigma_{s/a}$	ρ	ψ	β	v	S_c	$g(f)^1$, $S_c(f)^1$
Description	HTDMA	Tensiometer	Densitometer	Physical model (Wolf 2003)				
PAA (2 kg mol^{-1}, $f = 69.9$)	Brooks et al. (2004)	Fig. 9	1543 kg m^{-3} Tondre and Zana (1972)	$9.02 \cdot 10^{-3}$	-0.306	0.922	Fig. 5	Figs 1, 6
PEG (0.6 kg mol^{-1}, $f = 33.3$)	Fig. 1	Couper and Eley (1948)	1123 kg m^{-3} Eliassi and Modarress (2005)	$8.86 \cdot 10^{-3}$	-0.235	0.942	—	Fig. 1

[1]Requires the additional assumption that $\chi(\phi)$ is not a function of polymer chain length.
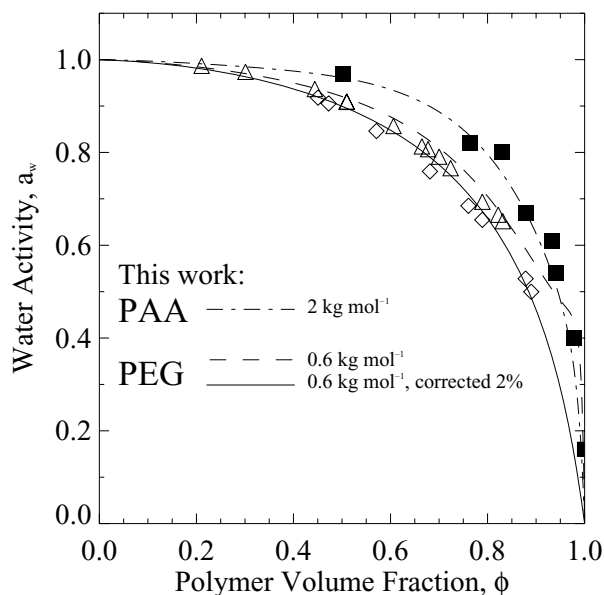
Fig. 3. Water activity measurements of PEG ($\triangle$ 0.6 kg mol^{-1}, $T =$ 313.15 K; $\diamond$ 0.6 kg mol^{-1}, $T = 293.15$ K) by Gaube et al. (1993) and PAA ($\blacksquare$ 4.0 kg mol^{-1}, $T = 298$ K) by Safronov et al. (1993). Water activity, inferred from Figure 1, for PEG, corrected PEG (assuming that the dry diameter was biased low by 2%), and PAA is also shown. PEG and PAA weight fractions were converted to volume fractions using dry density values from Eliassi and Modarress (2005) and Tondre and Zana (1972), respectively.

Fig. 4. Measured activated fraction for a dry 0.097 μm diameter PAA (2 kg mol^{-1}) particle. Vertical lines show $\pm$ 1 standard deviation of the measurement. The shaded region represents the overall uncertainty of our experimental determination of S_c.

(2005). In this mole-fraction based approach, the composition-dependence of $\nu\Phi$ (*cf*. Appendix A.1) is modelled by a second-order polynomial. Formally, the Kreidenweis et al. (2005) model is defined by $D/D_{\text{dry}} = [1 + (a + ba_w + ca_w^2)\frac{a_w}{1-a_w}]^{\frac{1}{3}}$, eq. (3) and the surface tension relationship developed in Appendix A.3. Here a, b and c are fitted coefficients obtained from hygroscopic growth factor data. Figure 5 shows that the Kreidenweis et al. (2005) model produces a very similar result when compared to that obtained by FHK theory. However it represents only the compound molecular weight that the fitting was performed for and cannot capture variations in water content with molecular weight as Flory–Huggins theory does.

The growth factor at $RH = 85\%$ and the critical supersaturation of dry 0.1 μm diameter PAA particles are predicted to depend on the chain segment number (the degree of polymerization), f, as shown in Fig. 6, where we have assumed that our χ-ϕ expression [Fig. 2, eq. (2)] derived for a molecular weight of 2 kg mol^{-1} applies for all degrees of polymerization. When $f > 15$, corresponding to molecular weights exceeding 0.4 kg mol^{-1}, FHK theory predicts that the hygroscopic growth factor becomes nearly constant, whereas it monotonically approaches unity (non-hygroscopic particles) for RK theory. In contrast, although f is an important determinant for water uptake in more dilute solutions, it only moderately affects the critical supersaturation. This result suggests that aging of atmospheric organic par-
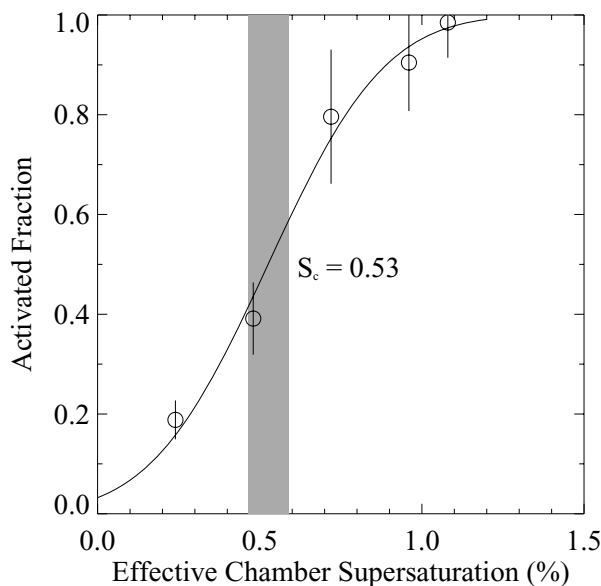
ticles involving increases in the extent of polymerization makes them poorer cloud condensation nuclei, but to a lesser extent than anticipated by RK theory. The similarity of the critical supersaturations predicted by FHK and RK theory can be explained as follows: as the particle grows in size and dilutes, the volume fraction of polymer becomes small, water activity approaches unity, and the terms in eq. (1) involving f and χ become less important. Nevertheless, RK theory underpredicts the aerosol water content (relative to FHK theory) at all volume fractions shown in Fig. 5. The underprediction of the water content leads to an enhanced Kelvin effect due to the smaller droplet diameter, which is partially compensated by the reduced water activity (and reduced surface tension) at larger polymer volume fraction.

The trends anticipated by FHK theory shown in Fig. 6 are consistent with the observed temporal evolution of the cloud condensation nucleus activity of SOA aerosol (VanReken et al., 2005), and with the relative constancy of hygroscopic growth factors (Baltensperger et al., 2005) of such particles during progressive polymerization.

4. Discussion

In our approach, summarized in Table 1, we have relied on measured hygroscopic growth factors. These data were converted to an effective, composition-dependent, Flory–Huggins interaction parameter and the result was fit to the three parameter model developed by Wolf (2003). This model can explain the insensitivity of the hygroscopic growth factor to molecular size. The same finding has also been noted by McFiggans et al. (2005),
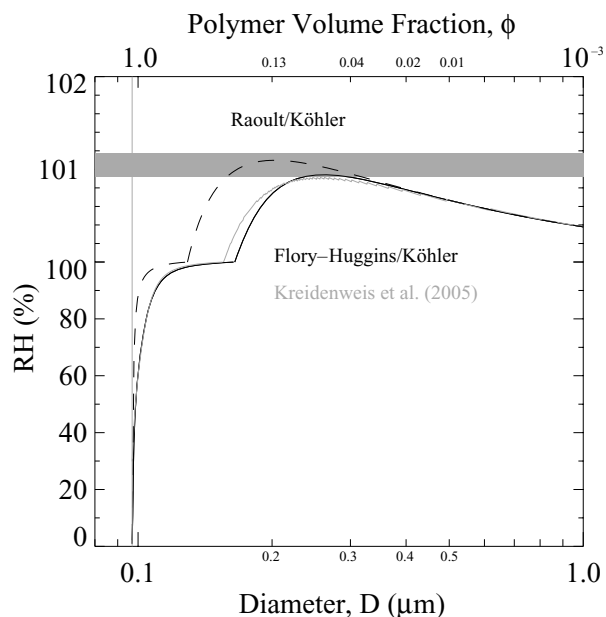
Fig. 5. Köhler curves for PAA (2.0 kg mol^{-1}) calculated based on FHK (solid) and RK (dashed) theory, for a dry diameter of 0.097 μm (vertical line). Results for the Kreidenweis et al. (2005) model are also shown. The FHK calculations use the ϕ-χ relationship shown in Fig. 2. In all calculations we use composition-dependent values of surface tension (Appendix A.3). The shaded region represents the measured critical supersaturation. Predicted supersaturations are $S_c = 0.47\%$ (FHK), $S_c = 0.46\%$ (Kreidenweis) and $S_c = 0.55\%$ (RK).

but their explanation is based on a modified version of the UNI-FAC model (Topping et al., 2005). This type of model predicts water activity based on a set of fitted parameters that model the interaction between functional groups and solvent molecules. The UNIFAC approach is in contrast to Flory–Huggins theory, which in its simplest form, that is, when a constant interaction parameter is used, assumes that the water activity is a colligative property and, therefore, depends only on the quantity and size (or space occupied in the solvent matrix) of the macromolecule. Interactions between functional groups and solvent molecules are accounted for in the model developed by Wolf (2003) but models that predict the Flory interaction parameter, and its variation with composition, based on functional group data are not available to date.

In constructing Fig. 6, we have not considered miscibility gaps, which are observed when a binary polymer–water system is cooled below the temperature of incipient phase separation (critical point). This behaviour is illustrated in the schematic phase diagram, shown in Fig. 7. The miscibility gap of polymer solutions is asymmetric, with the critical point skewed toward more dilute compositions (Flory, 1953). The co-existence, or binodal curve, describes the phase boundary and envelops the metastable limit, or spinodal curve. For a bulk solution at constant temperature, two binodal points define the volume frac-
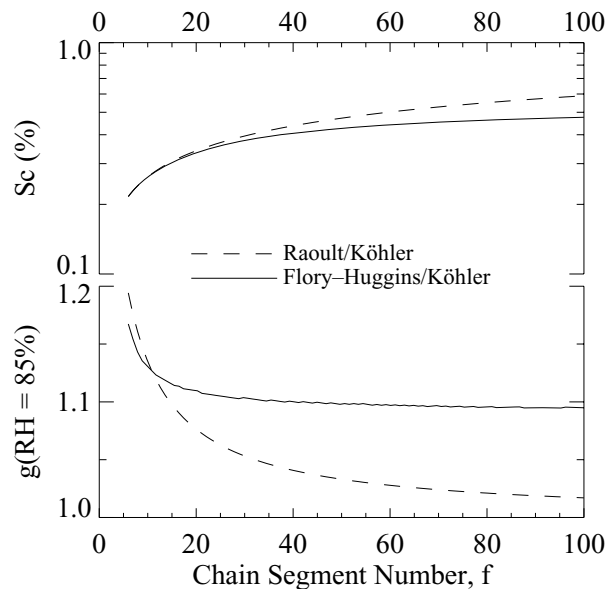

Fig. 6. Sensitivity of the hygroscopic growth factor (bottom) and the critical supersaturation (top) of PAA to the chain segment number, f, assuming a dry spherical 0.1 μm diameter particle. Calculations are as in Fig. 3.
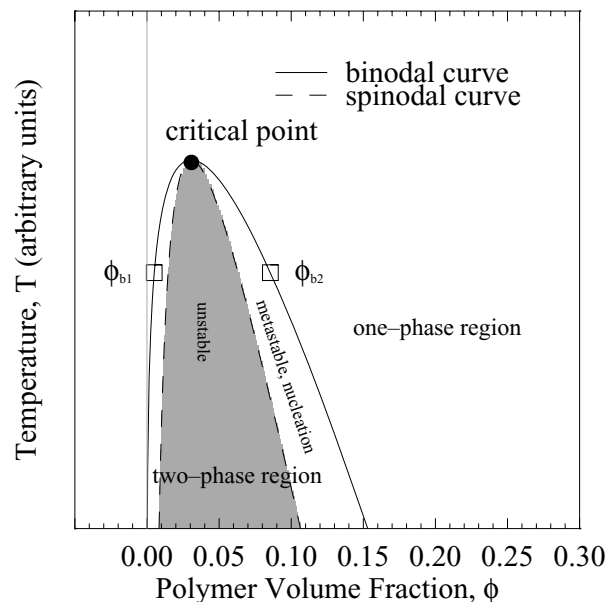

Fig. 7. Schematic phase diagram for an aqueous polymer solution.

tions of two co-existing phases, one with a more dilute volume fraction, ϕ_{b1}, and the other with a more concentrated volume fraction, ϕ_{b2}, that are in thermodynamic equilibrium and have the same water activity. Overall solution volume fractions below the binodal curve, that is, $\phi_{b1} < \phi < \phi_{b2}$ partition into two aqueous phases, with the relative amounts of each phase being dictated by the well-known lever rule. Phase decomposition is spontaneous inside the spinodal envelope, whereas phase nucleation is required to initiate phase separation in solutions with

compositions between the binodal and spinodal curves, shown as the metastable region in the diagram.

We now consider the possible equilibrium states of an atmospheric particle with limited miscibility, having a phase diagram similar to that shown in Fig. 7. In the atmosphere, an additional phase is present and must be considered, namely the vapour. We assume the polymer is non-volatile, and so only water establishes equilibrium with the environment. We further assume that the particle approaches the two-phase region from the more concentrated region, that is, from a lower RH region into a higher RH region. Under the typical assumptions used in the development of Köhler theory, the equilibrium condition just before phase separation is

$$RH_{\phi_{b2}}/100 = a_{\rm w}(\phi_{b2}) \exp\left(\frac{A}{D_{dry}}\phi_{b2}^{1/3}\right), \qquad (4)$$

where $A = (4\sigma_{\rm s/a}M_{\rm w})/(\rho_{\rm w}RT)$ and $D_{\rm dry}$ is the dry particle diameter. If the environmental RH is raised just *above* that required to maintain a stable equilibrium at ϕ_{b2}, the only possible equilibrium state of the particle is a single-phase solution having composition more dilute than ϕ_{b1}. This further dilution is necessary because, as is shown in Fig. 8, the environmental RH required for equilibrium for a particle of composition ϕ_{b1} is lower than that at ϕ_{b2}. This occurs because, although the water activities are

Fig. 8. Particle growth and equilibria expressed in water activity-composition space. For illustrative purposes, the water activity of 0.9999995 and the compositions ϕ_{b1} and ϕ_{b2} were predicted based on Flory–Huggins theory, eq. (4), assuming a constant $\chi = 0.54$ and $f = 1000$. Water activities are equal at the two binodal volume fractions, but the relative humidity over the two different-sized droplets is not. Hygroscopic growth factors g were calculated from polymer volume fractions and relative droplet sizes at ϕ_{b1} and ϕ_{b2} are drawn to scale.

equal for both compositions, the Kelvin term is reduced for the larger particle. Equilibrium considerations thus predict that only a dilute, single-phase, large particle can exist if the environmental RH is raised above that required at ϕ_{b2}, and from a kinetic standpoint, dilution is favoured because raising the environmental RH creates a driving force for condensation of water onto the particle.

We note that the transition between ϕ_{b2} and ϕ_{b1} is a phase change analogue to particle deliquescence. If the deliquescence RH is larger than the traditional Köhler maximum, then the particle will simultaneously undergo cloud droplet activation (e.g. Bilde and Svenningsson, 2004). This analogy holds for polymers with a miscibility gap. If the composition at ϕ_{b1} is sufficiently dilute, corresponding to water activity across the miscibility gap that is very close to unity, then the RH that is necessary to establish equilibrium at ϕ_{b2} may be supersaturated beyond the traditional Köhler maximum and, in that case, the particle should undergo cloud droplet activation.

It is not known if aqueous solutions of atmospherically relevant polymers exhibit miscibility gaps, and, if so, at which temperatures and compositions. Further studies are needed to establish the validity of the idea that cloud droplet activation may occur at the point of incipient phase separation.

5. Conclusions

Laboratory studies show that for two commercial polymers, PEG and PAA, hygroscopic growth factors did not depend on the degree of polymerization, and were larger than expected for such high-molecular-weight species. This behaviour is consistent with polymer-water interactions, as described by Flory–Huggins theory. By combining Flory–Huggins and Köhler theories, and also accounting for surface tension lowering effects, we show that hygroscopic growth factors are expected to be only a weak function of the extent of polymerization. This prediction is consistent with our laboratory data and with the time variation of the reported water uptake of continuously polymerizing SOA measured by Baltensperger et al. (2005). On the other hand, the theory predicts that molecular weight has a measurable influence on the cloud-nucleating activity of polymer solutions. A decrease in CCN activity with increasing molecular weight was also inferred by VanReken et al. (2005) from measurements on SOA. We experimentally confirmed the agreement between measured critical supersaturations of ~0.1 μm particles and the predictions based on parameters derived by fitting hygroscopic response to Flory–Huggins theory.

The polymers that we have tested so far were soluble in water in all proportions. However, in general, polymer solubility is expected to vary with the extent of polymerization, with temperature, and also with the addition of inorganic salts. If aqueous solutions of polymers found in atmospheric aerosols are not miscible for some dilute compositions, as is frequently found for manufactured polymers, then cloud droplet activation might proceed
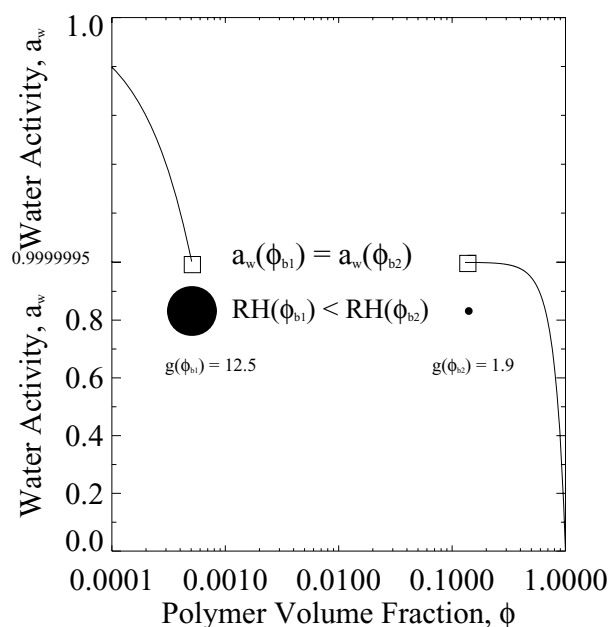
through a non-classical pathway, occurring not at the critical supersaturation, but at the saturation ratio needed to establish equilibrium with a single-phase droplet having a composition equal to the miscibility limit of water in the polymer. Further research into the nature of oligomers and polymers present in the ambient aerosol and their phase diagrams, including behaviour in mixed particles, is required to better understand their role in cloud droplet formation.

6. Acknowledgments

7. Appendix A

A.1 Raoult Köhler Theory

The water activity, parametrized based on Raoult's law, is (Pruppacher and Klett, 1997),

$$a_w = \left(1 + \nu \Phi \frac{n_s}{n_w}\right)^{-1} \qquad (A1)$$

where a_w is the water activity, ν is the number of soluble ions (assumed to be unity for weakly dissociating polymers such as PAA, *cf.* Appendix A.2), Φ is the molal osmotic coefficient of the solute in solution (commonly assumed to be unity for dilute systems), n_s is the number of moles of solute, and n_w is the number of moles of water. We have applied the common assumption that the volume change of mixing is zero. Equations (3) and (A1) (and including composition dependent surface tension described in Appendix A.3) define what we call Raoult/Köhler or RK theory.

A.2 pH Measurement

PAA is a weak polyacid and thus lowers the pH of the solution. For pure polyacids, a simple logarithmic dependence of pH with composition is expected for the entire concentration range (Maeda and Oosawa, 1972). We measured the pH using an ORION Model 250A glass electrode and found that pH = $2.87 - 0.20 \ln(X)$ for $0.01 < X < 5$, where X denotes the weight percent (wt%) of PAA (2 kg mol^{-1}) in aqueous solution. These measurements demonstrate that the degree of dissociation is small. The degree of dissociation can be estimated by dividing $c_{H^+} \approx 10^{-pH}$ by the number of moles of dissociable groups. For $X = 10$ wt% PAA (2 kg mol^{-1}), this ratio is ~0.003, indicat-

ing that 3 out of 1000 carboxyl groups dissociated ($\nu \approx 1.08$). Therefore, we conclude the effect of ionization of the functional groups on the water activity (Warren, 1997) can also be neglected to a first approximation.

A.3 Surface Tension

To accurately predict S_c we measured the surface tension of bulk PAA solutions as a function of composition using a CENCO-DuNouy Tensiometer. The measured surface tension of deionized water (Barnsted NANOPure, 18.2 MΩ) was 0.0699 ± 0.008 J m^{-2}, 4% lower than the accepted value of 0.0730 J m^{-2} at $T = 293$ K (Pruppacher and Klett, 1997). To account for this bias, we parametrize our composition dependent values relative to the measured value of pure water.

$$f_s = 1 + a_1 \ln(a_2 X + 1) \qquad (A2)$$

where f_s is the fractional surface tension (normalized with respect to pure water), X denotes weight percent of solute, and a_1, a_2 are fitted coefficients. The surface tension of the solution is given by

$$\sigma_{s/a} = \sigma_{w/a,T} \cdot f_s \qquad (A3)$$

where $\sigma_{w/a,T}$ is the surface tension for pure water at temperature T (Pruppacher and Klett, 1997). Although PEG is only slightly surface active (Couper and Eley, 1948), we found that PAA significantly lowered the surface tension (Fig. 9). According to FHK theory $X = 7.8\%$ at activation for PAA. For more concentrated solutions, we expect that the error incurred from extrapolating
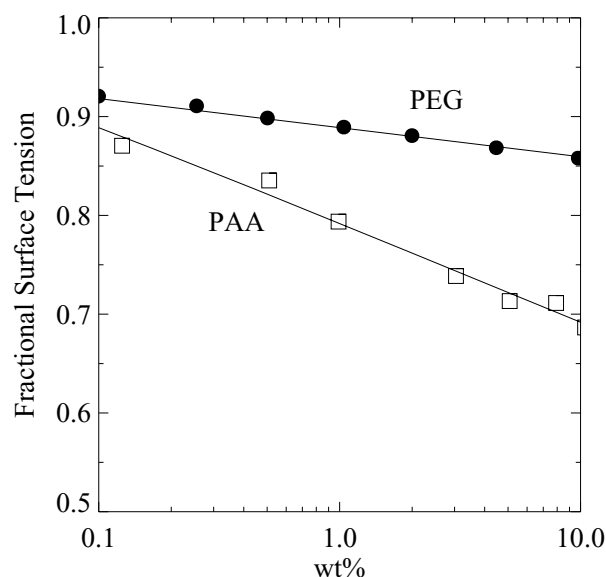

Fig. 9. Fractional surface tension for PAA ($\Box$, 2 kg mol^{-1}, $a_1 = -0.0435$, $a_2 = 119$) and PEG ($\bullet$, 1 kg mol^{-1}, $a_1 = -0.0128$, $a_2 = 5890$). PEG data are from Couper and Eley (1948).

Equation (A.2) to beyond the range of measured values is small because the logarithmic slope is expected to be extended from theoretical considerations (Couper and Eley, 1948).

References

Baltensperger, U., Kalberer, M., Dommen, J., Paulsen, D., Alfarra, R. and co-authors. 2005. Secondary organic aerosols from anthropogenic and biogenic precursors. *Faraday Discuss.* **130**, 1–14.

Brandrup. *Polymer Handbook*, (eds.Brandrup J., Immergut, E. H., and Grulke, E. A.), John Wiley & Sons, INC., New York, NY.

Bilde, M. and Svenningsson, B. 2004. CCN activation of slighlty soluble organics: the importance of small amounts of inorganic salt and particle phase. *Tellus* **56B**, 128–134.

Brechtel, F. J. and Kreidenweis, S. M. 2000. Predicting particle critical supersaturation from hygroscopic growth measurements in the humidified TDMA. Part II: Laboratory and ambient studies. *J. Atmos. Sci.* **57**, 1872–1887.

Brooks, S. D., DeMott, P. J. and Kreidenweis, S. M. 2004. Water uptake by particles containing humic materials and mixtures of humic material with ammonium sulfate. *Atmospheric Environment* **38**, 1859–1868.

Carrico, C. M., Kreidenweis, S. M., Malm, W. C., Day, D. E., Lee, T. and co-authors. 2005. Hygroscopic growth behaviour of carbon-dominated aerosol in Yosemite National Park. *Atmos. Environ.* **39**, 1392–1404.

Chan, M. N. and Chan, C. K. 2003. Hygroscopic properties of two model humic-like substances and their mixtures with inorganics of atmospheric importance. *Environ. Sci. Technol.* **37**, 5109–5115.

Cini, R., Innocenit, N. D., Loglio, G., Oppo, C., Orlandi, G. and co-authors. 1996. Air-sea exchange: sea salt and organic microcomponents in Antarctic snow. *Int. J. Environ. Ana. Chem.* **63**, 15–27.

Couper, A. and Eley, D. 1948. Surface tension of polyoxyethylene glycol solutions. *J. Poly. Sci.* **3**, 345–349.

Decesari, S., Facchini, M. C., Matta, E., Lettini, F., Micea, M. and co-authors. 2001. Chemical features and seasonal variation of fine aerosol water-soluble organic compounds in the Po valley. *Atmos. Environ.* **36**, 1827–1332.

Eliassi, A. and Modarress, H. 2005. Excess volume of polymer/solvent mixtures and proposed model for prediction of activity of solvents based on excess volume data. *J. Appl. Poly. Sci.* **95**, 1219–1227.

Facchini, M. C., Mircea, M., Fuzzi, S. and Charlson, R. J. 1999. Cloud albedo enhancement by surface-active organic solutes in growing droplets. *Nature* **401**, 257–259.

Feng, J. S. and Möller, D. 2004. Characterization of water-soluble macromolecular substances in cloud water. *J. Atmos. Chem.* **48**, 217–233.

Flory, P. J. 1953. *Principles of Polymer Chemistry*, Cornell University Press, Ithaca, NY.

Gao, S., Ng, N. L., Keywood, M., Varutbangkul, V., Bahreini, R. and co-authors. 2004. Particle phase acidity and oligomer formation in secondary organic aerosol. *Environ. Sci. Technol.* **38**, 6582–6589.

Gaube, J., Pfennig, A. and Stumpf, M. 1993. Vapor-liquid-equilibrium in binary and ternary aqueous-solutions of poly(ethylene glycol) and dextran. *J. Chem. Engin. Data* **38**, 163–166.

Gysel, M., Weingartner, E., Nyeki, S., Paulsen, D., Baltensperger, U. and co-authors. 2004. Hygroscopic properties of water-soluble matter and humic-like organics in atmospheric fine aerosol. *Atmos. Chem. Phys.* **4**, 35–50.

Herckes, P., Lee, T., Trenary, L., Kang, G., Chang, H. and Collet Jr., J. L. 2002. Organic matter in central California radiation fogs. *Environ. Sci. Technol.* **36**, 4777–4782.

IPCC. *Climate Change 2001: The Scientific Basis. Contribution of the Working Group I to the Third Assessment Report of the Intergovernmantal Panel on Climate Change*, (eds. Houghton J. T., Ding, Y., Griggs, D. J., Noguer, M., van der Linden, P. J. and co-authors. Cambridge University Press, New York, NY.

Kalberer, M., Paulsen, D., Sax, M., Steinbacher, M., Dommen, J. and co-authors. 2004. Identification of polymers as major components of atmospheric organic aerosols. *Science* **303**, 1659–1662.

Kreidenweis, S. M., Koehler, S. M., DeMott, P. J., Prenni, A. J., Carrico, C. and co-authors. 2005. Water activity and activation diameters from hygroscopicity data—Part I: Theory and application to inorganic salts. *Atmos. Chem. Phys.* **5**, 1357–1370.

Langmuir, I. 1917. The constitution and fundamental properties of solid and liquids. II. Liquids.. *J. Amer. Chem. Soc.* **39**, 1848–1906.

Limbeck, A., Kulmala, M. and Puxbaum, H. 2003. Secondary organic aerosol formation in the atmosphere via heterogeneous reaction of gaseous isoprene. *Geophys. Res. Lett.* **30**, 1996, doi:10.1029/2003GL017738.

Maeda, H. and Oosawa, F. 1972. A theory for the dependence of pH on polyelectrolyte concentration. *J. Phys. Chem.* **76**, 3445–3450.

Manahan S. E. *Environmental Chemistry*, Lewis Publishers, New York, NY.

McFiggans, G. B., Alfarra, M. R., Allan, J., Bower, K., Coe, H. and co-authors. 2005. Simplification of the representation of the organic component of atmospheric particulates. *Faraday Discuss.* **130**, 1–22.

Mochida, M. and Kawamura, K. 2004. Hygroscopic properties of levoglucosan and related organic compounds characteristic to biomass burning aerosol particles. *J. Geophys. Res.* **109**, 21202, doi:10.1029/2004JD004962.

Prausnitz, J. M., Lichtenthaler, R. N. and Azevedo, E. G. 1999. *Molecular Thermodynamics of Fluid-Phase Equilibria*, Prentice Hall, Upper Saddle River, NJ.

Prenni, A. J., DeMott, P. J. and Kreidenweis, S. M. 2003. Water uptake of internally mixed particles containing ammonium sulfate and dicarboxylic acids. *Atmos. Environ.* **37**, 4243–4251.

Pruppacher, H. R. and Klett, J. D. 1997. *Microphysics of Clouds and Precipitation*, Kluwer Academic Publishers, Dordrecht.

Rader, D. J. and McMurry, P. H. 1986. Application of the tandem differential mobility analyzer to studies of droplet growth or evapouration. *J. Aerosol Sci.* **17**, 771–787.

Raatikainen, T. and Laaksonen, A. 2005. Application of several activity coefficient models to water-organic-electrolyte aerosols of atmospheric interest. *Atmos. Chem. Phys. Disc.* **5**, 3641–3699.

Safronov, A. P., Tager, A. A., Klyuzhin, E. S. and Adamova, L. V. 1993. Thermodynamics of the interaction of polyacrylic-acid with water. *Vysokomolekulyarnye Soedineniya* **35**, A700–A704.

Seinfeld, J. H. and Pandis, S. N. 1998. *Atmospheric Chemistry and Physics*, John Wiley & Sons, INC., New York.

Snider, J. R., Guibert, S. and Brenguier, J. L. 2003. Aerosol activation in marine stratocumulus clouds: 2. Köhler and parcel theory closure studies. *J. Geophys. Res.* **108**, 8629, doi:10.1029/2002JD002692.

Tondre, C. and Zana, R. 1972. Apparent molal volumes of polyelectrolytes in aqueous solutions. *J. Phys. Chem.* **76**, 3451–3459.

Topping, D. O., McFiggans, G. B. and Coe, H. 2005. A curved multi-component aerosol hygroscopicity model framework: Part 2 - Including organic compounds. *Atmos. Chem. Phys.* **5**, 1223–1242.

VanReken, T. M., Ng, N. L., Flagan, R. C. and Seinfeld, J. H. 2005. Cloud condensation nucleus activation properties of biogenic organic aerosol. *J. Geophys. Res.* **110**, D07206, doi:10.1029/2004JD005465.

Warren, P. B. 1997. Simplified mean field theory for polyelectrolyte phase behaviour. *J. Physique II* **7**, 343–361.

Wolf, B. A. 2003. Chain connectivity and conformational variability of polymers: Clues to an adequate thermodynamic description of their solutions, 2 Composition dependence of the Flory–Huggins interaction parameters. *Macromol. Chem. Phys.* **204**, 1381–1390.

Zhou, J., Swietlicki, E., Hansson, H. C. and Artaxo, P. 2002. Submicrometer aerosol particle size distribution and hygroscopic growth measured in the Amazon rain forest during the wet season. *J. Geophys. Res.* **107**, 8055, doi:10.1029/2000JD000203.